



RESEARCH ARTICLE

Multi-parametric quantitative magnetic resonance imaging of the upper arm muscles of patients with spinal muscular atrophy

Melissa T. Hooijmans¹  | Laura E. Habets² | Sandra A. M. van den Berg-Faay¹ |
 Martijn Froeling³  | Fay-Lynn Asselman⁴ | Gustav J. Strijkers⁵ |
 Jeroen A. L. Jeneson² | Bart Bartels² | Aart J. Nederveen¹ | W. Ludo van der Pol⁴

¹Department of Radiology and Nuclear Medicine, Amsterdam Movement Sciences, Amsterdam University Medical Center, Amsterdam, The Netherlands

²Center for Child Development, Exercise and Physical Literacy, Wilhelmina Children's Hospital, University Medical Center Utrecht, Utrecht, The Netherlands

³Department of Radiology, University Medical Center Utrecht, Utrecht, The Netherlands

⁴UMC Utrecht Brain Center, Department of Neurology and Neurosurgery, University Medical Center Utrecht, Utrecht University, Utrecht, The Netherlands

⁵Department of Biomedical Engineering and Physics, Amsterdam Movement Sciences, Amsterdam University Medical Center, Amsterdam, The Netherlands

Correspondence

Melissa T. Hooijmans, Department of Radiology and Nuclear Medicine, ZO-174, AUMC, Meibergdreef 9, 1105 AZ, Amsterdam, The Netherlands.

Email: m.t.hooijmans@amsterdamumc.nl

Funding information

Prinses Beatrix Spierfonds; Grant/Award Number: W.OR17-05. Stichting Spieren voor Spieren. Zwaluwen Jeugd Actie.

Quantitative magnetic resonance imaging (qMRI) is frequently used to map the disease state and disease progression in the lower extremity muscles of patients with spinal muscular atrophy (SMA). This is in stark contrast to the almost complete lack of data on the upper extremity muscles, which are essential for carrying out daily activities. The aim of this study was therefore to assess the disease state in the upper arm muscles of patients with SMA in comparison with healthy controls by quantitative assessment of fat fraction, diffusion indices, and water T2 relaxation times, and to relate these measures to muscle force. We evaluated 13 patients with SMA and 15 healthy controls with a 3-T MRI protocol consisting of DIXON, diffusion tensor imaging, and T2 sequences. qMRI measures were compared between groups and related to muscle force measured with quantitative myometry. Fat fraction was significantly increased in all upper arm muscles of the patients with SMA compared with healthy controls and correlated negatively with muscle force. Additionally, fat fraction was heterogeneously distributed within the triceps brachii (TB) and brachialis muscle, but not in the biceps brachii muscle. Diffusion indices and water T2 relaxation times were similar between patients with SMA and healthy controls, but we did find a slightly reduced mean diffusivity (MD), λ_1 , and λ_3 in the TB of patients with SMA. Furthermore, MD was positively correlated with muscle force in the TB of patients with SMA. The variation in fat fraction further substantiates the selective

Abbreviations used: BB, biceps brachii; BR, brachialis; DMD, Duchenne muscular dystrophy; DTI, diffusion tensor imaging; FA, fractional anisotropy; FF, fat fraction; FSHD, facioscapulohumeral muscular dystrophy; HCs, healthy controls; HFMSE, Hammersmith Functional Motor Scale Expanded; MD, mean diffusivity; MRC, Medical Research Council; MVCF, maximal voluntary contraction force; qMRI, quantitative magnetic resonance imaging; qT2, quantitative T2; SMA, spinal muscular atrophy; SMN, survival motor neuron; SNR, signal-to-noise ratio; SPAIR, SPectral Adiabatic Inversion Recovery; SPIR, Spectral Presaturation with Inversion Recovery; SSGR, slice-selective gradient reversal; TB, triceps brachii; λ_1 , eigenvalue 1; λ_2 , eigenvalue 2; λ_3 , eigenvalue 3.

This is an open access article under the terms of the [Creative Commons Attribution-NonCommercial](https://creativecommons.org/licenses/by-nc/4.0/) License, which permits use, distribution and reproduction in any medium, provided the original work is properly cited and is not used for commercial purposes.

© 2022 The Authors. *NMR in Biomedicine* published by John Wiley & Sons Ltd.

vulnerability of muscles. The reduced diffusion tensor imaging indices, along with the positive correlation of MD with muscle force, point to myofiber atrophy. Our results show the feasibility of qMRI to map the disease state in the upper arm muscles of patients with SMA. Longitudinal data in a larger cohort are needed to further explore qMRI to map disease progression and to capture the possible effects of therapeutic interventions.

KEYWORDS

quantitative magnetic resonance imaging, skeletal muscle, spinal muscular atrophy, upper arm muscles

1 | INTRODUCTION

Spinal muscular atrophy (SMA) is caused by homozygous loss of function of the *SMN1* gene.^{1,2} The deficiency of survival motor neuron (SMN) protein results in extensive changes in the motor unit, including loss of alpha-motor neurons, abnormal anatomy of the neuromuscular junction, and progressive muscle wasting, and is characterized by predominant axial and proximal muscle weakness.^{1,3,4} SMA has a wide range of severity from lethal neonatal to adult symptom onset. This variation is reflected in the clinical classification system that distinguishes four types based on the achieved motor milestones, sitting and walking, and the age of disease onset.^{5,6} An increasing number of genetic therapies that increase cellular SMN protein levels have obtained market authorization.^{7,8} With these already available therapeutic strategies and emerging second-generation therapies that also directly target muscle, quantitative outcome measures are of increasing importance. Ideally, these outcome measures have a broad dynamic range and reflect disease state and progression over a wide range of disease stages.⁹

Quantitative magnetic resonance imaging (qMRI) has been used to map the natural disease progression in neuromuscular disorders, including SMA.^{10–12} The majority of imaging studies in SMA have focused on characterizing the progressive replacement of muscle tissue by fat, using both qualitative and quantitative mapping strategies.^{13–18} Fat fraction (FF), primarily assessed in the leg muscles, correlates with disease progression and functional outcomes in SMA.^{13,14,19} A few studies have also explored other pathophysiological processes, including inflammation using T2 mapping and changes in muscle microstructure using diffusion tensor imaging (DTI).^{11,12,19,20} This is in contrast to the almost complete lack of studies aiming to assess the disease state and progression in the arm muscles of patients with SMA. This is likely due to challenges inherent to imaging of the upper extremity muscles, such as respiratory motion, body positioning difficulties, and field inhomogeneity due to the off-center location of the upper arm. However, the muscles of the shoulder and upper arm are essential for carrying out daily activities, such as eating and personal care, and they remain preserved for a longer time compared with leg muscles.^{21,22} Consequently, quantitative measures of the upper extremity muscles are critical for meaningful disease markers across a wide range of disease stages.

Imaging data in patients with SMA, specifically FF, are commonly represented as an average over multiple central slices or a specific region, even although it is not known how fat is distributed within muscles. Recent studies in other neuromuscular diseases, including Duchenne muscular dystrophy (DMD), Becker muscular dystrophy (BMD), and facioscapulohumeral muscular dystrophy (FSHD),^{23–26} have shown that FF varies both within and between individual muscles. Hence, evaluation of the fat distribution in patients with SMA is necessary to provide insights into the selective vulnerability of extremity muscles in this patient population.

The primary aim of this study was to quantitatively assess FF, diffusion indices, and water T2 relaxation time in the upper arm muscles of patients with SMA in comparison with healthy controls (HCs). Furthermore, we investigated the distribution of FF within individual upper arm muscles in both patients with SMA and HCs. Lastly, we explored the associations of these quantitative MR outcome measures with functional measures in patients with SMA.

2 | METHODS

2.1 | Study population

Patients were recruited from the Dutch SMA registry (www.treatnmd.eu/patientregistries). All patients with SMA had a confirmed homozygous deletion of the *SMN1* gene or a heterozygous *SMN1* deletion in combination with a disabling point mutation on the second *SMN1* allele. We used the current SMA classification system with minor modifications, as described previously.²⁷ The inclusion criteria for this study were: (1) aged older than 12 years; (2) an ability to perform active arm cycling movements; (3) an ability to follow test instructions; and (4) a biceps brachii (BB) muscle Medical Research Council (MRC) score for muscle strength of 4 or higher, and a triceps brachii (TB) muscle MRC score of 2 or higher. The

exclusion criteria were: (1) contraindications concerning MRI assessment; (2) risk factors for exercise testing registered by a Dutch version of the Preparticipation Questionnaire (American College of Sports Medicine and American Heart Association); (3) mental retardation; (4) comorbidities affecting exercise tolerance; or (5) being under examination for a nondiagnosed disease at the time of the investigation. The measurements described in this study were part of a larger data collection, also investigating exercise intolerance, hence some of the inclusion criteria.^{28,29} We recruited control participants with the help of the patients' social network of family and friends and also via social media. The study was approved by the medical ethical committee of the University Medical Center of Utrecht (NL62792.041.17) and all the participants (and, if necessary, their parents) signed written informed consent.

2.2 | Study set-up and functional measures

The study consisted of two visits. During the first visit, we documented baseline characteristics, including the Hammersmith Functional Motor Scale Expanded (HFMSSE), the MRC score for muscle strength of the BB/brachialis (BR) and TB muscle, and the maximal voluntary contraction force (MVCF) of the flexor muscles (BB/BR) and TB muscle. The HFMSSE is an assessment tool of physical abilities in type 2 and 3 SMA, consisting of 33 items with a total achievable score of 66. The MRC score assesses muscle strength from grade 0 (no visible contraction) to grade 5 (normal). MVCF was measured with a handheld dynamometer using the break test with the elbow in 90° flexion and supination of the lower arm (MicroFET2, Hoggan Health Industries, Salt Lake City, UT). MR datasets were acquired during the second visit. The two visits were preferably scheduled 2–8 weeks apart to prevent fatigue as a consequence of an maximal arm cycling task, which was also part of the same study.²⁹

2.3 | MR examination

MR datasets were acquired in the right upper arm on a 3-T MR System (Philips, Ingenia, Best, The Netherlands) using a 16-element receiver coil (anterior) and the 12-element receiver coil built into the patient table (posterior). Participants were positioned on their right side head-first in the MR scanner to position the right upper arm in the most central location of the bore. Sand bags were placed next to the upper and lower arm to stabilize the position next to the upper body. The neck, back, and legs of each participant were supported based on individual preferences. The anterior coil was placed on top of the participant and it covered the full upper arm and shoulder region. The data were acquired in a transverse stack with a field of view (FOV) of 480 x 276 mm². The total duration of the imaging protocol was approximately 20 min and it contained four sequences:

- i. A four-point Dixon sequence to determine muscle FF (MS-FFE; TR/TE/ΔTE = 210/2.3/0.76 ms; four echoes; acquisition matrix = 184 x 320; voxel size = 1.5 x 1.5 x 6 mm³; no gap; number of slices = 33; SENSE 2; duration 2 min 37 s).
- ii. A spin-echo echo planar imaging (SE-EPI) sequence with diffusion weighting to quantify diffusion indices (TR/TE = 6600/57 ms; number of gradient directions = 56; b-values 0 (1), 1 (8), 5 (3), 10 (3), 20 (3), 50 (3), 100 (3), 200 (10), 400 (10), 600 (12) s/mm²; number of signal averages = 1; acquisition matrix = 92 x 160; voxel size = 3 x 3 x 6 mm³; number of slices = 33; no slice gap; SENSE = 1.9; a combination of three fat suppression techniques: SPectral Adiabatic Inversion Recovery [SPAIR] and slice-selected gradient reversal [SSGR] for the main aliphatic fat peak, and a Spectral Presaturation with Inversion Recovery [SPIR] pulse for the olefinic fat peak; partial Fourier factor = 0.73; duration 4 min 50 s).
- iii. Noise acquisition to determine the signal-to-noise ratio (SNR) of the diffusion data (SE-EPI, TR/TE = 6200/56 ms; b = 0 + dynamic noise; acquisition matrix = 92 x 160; voxel size = 3 x 3 x 6 mm³; no gap; number of slices = 33; SPAIR/SSGR/SPIR; SENSE = 1.9; partial Fourier factor = 0.73; duration 1 min 27 s).
- iv. A multiecho spin echo (MESE) sequence to measure water T2 relaxation times (TSE; TR/TE/ΔTE = 4000/7.7/7.6 ms; number of echoes = 17; acquisition matrix = 92 x 160; voxel size = 3 x 3 x 6 mm³; number of slices = 17; slice gap = 6 mm; flip angle/refocusing angle = 90°/180°; SENSE = 2; duration 6 min 24 s).

The middle of the slice stack of each of the sequences was positioned at midhumerus level, perpendicular to the humerus bone.

2.4 | MR data analysis

MR datasets were processed using QMRITools (<https://github.com/mfroeling/QMRITools>) for Wolfram Mathematica 11.3. The Dixon data were reconstructed using an iterative decomposition of water and fat with echo asymmetry and least-squares estimation (IDEAL) using eight reference fat peaks and considering a single T2* decay.³⁰ FF was calculated as the signal intensity (SI) fat/(SI fat + SI water) x 100. Contractile muscle volume (cVolume) was calculated as muscle volume x (100 - FF).

Diffusion data were denoised using a principal component analysis (PCA) noise algorithm and spatially registered to correct for motion- and eddy current-induced displacements using an open-source registration tool (<http://elastix.isi.uu.nl>).³¹ Furthermore, the diffusion data were registered to anatomical space using a rigid registration and a B-spline registration to correct for EPI distortions. The diffusion tensor was calculated using an intravoxel incoherent motion-based iterative weighted-linear-least-squares algorithm.³² The tensor was diagonalized, generating three eigenvectors and the corresponding eigenvalues (λ_1 , λ_2 , and λ_3) per voxel. Fractional anisotropy (FA) and mean diffusivity (MD) were calculated per voxel, based on the three eigenvalues, using standard equations. SNR levels were calculated per voxel based on the local average signal divided by the local noise sigma. DTI signal was determined on the $b = 0$ image, while the noise sigma was based on the DTI noise acquisition. Datasets with SNR levels of less than 10 or FF of more than 50% were excluded from the analysis.^{33,34}

Water T2 relaxation times were calculated using an extended phase graph (EPG) fitting approach, considering different T2 relaxation times for a single water and a single fat component. The fat calibration was performed per subject using 1000 random points automatically selected from the subcutaneous fat. The water T2 relaxation time, the FF, and the transmit field (B_1^+) were fitted on a voxel-by-voxel basis using a dictionary method. Pixels with a FF of more than 50%, based on the reconstructed FF map, were excluded from the analysis, as these pixels have been shown to impact the stability of the EPG fit.^{35,36}

Regions of interest (ROIs) were manually drawn on the reconstructed water image of the four-point Dixon sequence for the TB, BB, and BR muscle. ITK-snap (www.itksnap.org)³⁷ was used for the segmentation on the slices where the muscles were visible. FF, cVolume, water T2 relaxation time, MD, FA, λ_1 , λ_2 , and λ_3 are reported as mean values of all pixels in the ROI averaged over the full segmented volume. Additionally, the three upper arm muscles were divided into a distal, middle, and proximal segment (according to an equal number of slices per segment) to assess any potential differences in FF along the length of the individual upper arm muscles.

2.5 | Statistical analysis

Statistical analyses were performed using IBM SPSS (version 23; IBM Corp., Armonk, NY). Due to the low number of subjects and non-normal distributions, nonparametric tests were used for all analyses. Differences between HCs and patients with SMA for FF, cVolume, water T2 relaxation time, MD, FA, λ_1 , λ_2 , λ_3 , and MVCF were assessed using a Mann-Whitney U test. The level of statistical significance was corrected for multiple testing and p was set at 0.0055 or less (nine measures; $0.05/7 = 0.0055$). Furthermore, differences between the SMA types are described and visualized but were not tested due to the small group sizes. Differences in FF between muscle segments were evaluated using a Friedman test. The level of statistical significance was corrected for multiple comparisons and p was set at 0.008 or less (six comparisons; $0.05/6 = 0.0083$). A Wilcoxon signed-rank test was used as post hoc analysis to determine which of the muscle segments differed. Lastly, Kendall's tau correlation was used to explore the association between function measures (i.e. MVCF and HFMSE score) with four of the MR outcome measures, FF, MD, FA, and water T2 relaxation time in the patients with SMA. MVCF is measured for flexion and extension of the elbow. Elbow flexion MVCF is therefore associated with an average qMRI measure of the BR and BB muscle, as both muscles contribute to flexion force. The strengths of the associations are based on Kendall's tau coefficient and are classified as very weak ($\tau < 0.3$), weak ($0.3 < \tau < 0.5$), moderate ($0.5 < \tau < 0.7$), and strong ($\tau > 0.7$).

3 | RESULTS

3.1 | Study population

A total of 13 patients with SMA (median age: 47 years; range: 12–63 years; male/female: 5/8) and 15 HCs (median age: 38 years; range: 13–63 years; male/female: 6/9) participated in this study. The patient group consisted of patients with SMA type 3a (n: 4; median age: 31 years; range: 12–57 years), type 3b and type 4 (n: 9; median age: 54 years; range: 19–63 years). Because of the very low number of patients (i.e. one) with SMA type 4 in our study population, patients with SMA types 3b and 4 were grouped together when describing differences in qMRI outcome parameters between SMA types. All control and patient characteristics and function measures are reported in Table 1. Notable is the wide range of MVCF in the flexor muscles of the patients with SMA. MVCF was significantly lower in the flexor muscles ($Z = -3.7$; $p < 0.0001$) and TB muscle ($Z = -3.7$; $p < 0.0001$) in patients with SMA compared with HCs.

3.2 | Data quality and exclusion

For the DTI data, a total of 17 muscles were excluded (SMA: 12; HCs: 5). Of those 17 muscles, seven muscles (of four subjects) were excluded because their FF was more than 50% (SMA TB: 4; BB: 3). Additionally, DTI datasets of four muscles (of three subjects) were excluded due to

TABLE 1 Patients' characteristics

	SMA (n = 13)	Healthy controls (n = 15)
Age in years, median (min–max)	47 (12–63)	38 (13–63)
Sex (M/F)	5/8	6/9
MRC score BB, median (min–max)	4 (4–5)	5 (5–5)
MRC score TB, median (min–max)	4 (2–5)	5 (5–5)
HFMSE, median (min–max)	42 (11–65)	n.a.
MVCF flexor muscles, median (min–max)	119.6 (16–351.9)*	189.5 (114.3–437.3)
MVCF TB muscle, median (min–max)	29.1 (8.8–128.1)*	129.9 (95.2–250.4)

Notes: MRC score for muscle strength (right BB/BR and TB muscle); range between 0–5, HFMSE, 33 items with a total score of 66; MVCF measured in Newtons (N).

Abbreviations: BB, biceps brachii; BR, brachialis; HFMSE, Hammersmith Functional Motor Scale Expanded; MVCF, Maximal Voluntary Contraction Force; MRC, Medical Research Council; TB, triceps brachii.

*significant difference between patients and controls.

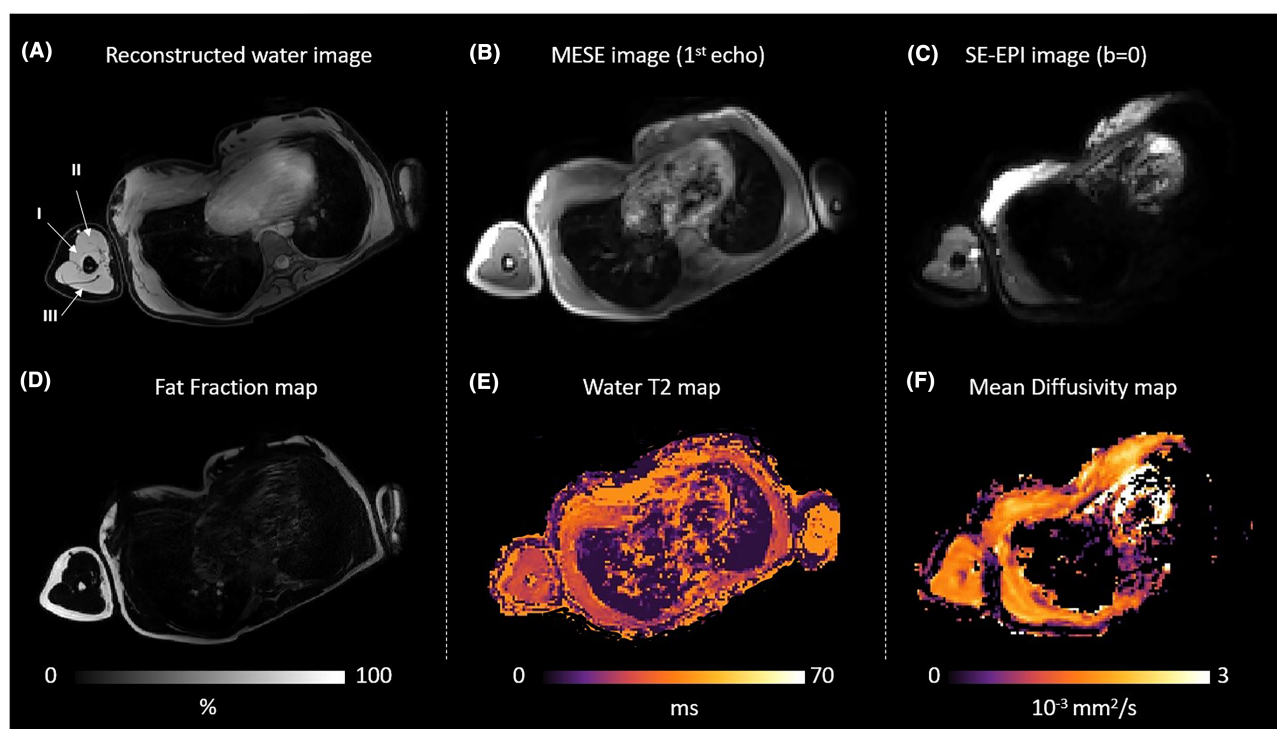


FIGURE 1 Multi-parametric axial images of the upper arm of a patient with spinal muscular atrophy. (A) An offline reconstructed water map of the Dixon scan on which the brachialis (I), biceps brachii (II), and triceps brachii (III) muscle are indicated. (B) First echo of a multiecho spin-echo (MESE) image and (C) A spin-echo echo planar imaging (SE-EPI) image without diffusion weighting ($b = 0$ s/mm²). (D) A reconstructed fat fraction map, (E) A reconstructed water T2 map, and (F) A reconstructed mean diffusivity (MD) map

insufficient SNR(<10) (SMA TB: 1, BB: 1, BR: 1; HC BB: 1), and six muscles (of three subjects) were excluded due to fat artefacts (SMA TB 1, BB: 0, BR: 1; HC TB: 1, BB: 2, BR: 1). All Dixon datasets were included for analysis and one T2 patient dataset was excluded due to data export problems.

3.3 | FF, cVolume, diffusion indices, and water T2 relaxation times

Multiparametric axial images of a representative patient with SMA are shown in Figure 1. The median, min, and max values for MVCF and MR outcome measures are summarized per group on a muscle-by-muscle basis in Table 2. Muscle FF was significantly higher in all upper arm muscles of patients with SMA compared with HCs ($Z > -2.76$; $p \leq 0.006$) (Figure 2). cVolume was significantly lower in the TB muscle of patients with SMA compared with HCs ($Z = -3.4$; $p = 0.0003$), while nonsignificant but slightly lower cVolumes were seen in BB ($Z = -2.004$; $p = 0.046$) and

TABLE 2 Quantitative magnetic resonance imaging outcome measures

Muscle	Parameter	SMA	Healthy controls	p value
Brachialis		N (FF/qT2) = 13/12	N = 15	
	Fat fraction (%)	13 (4.1–41.9)*	7.8 (6.8–11.8)	0.004
	Water T2 (ms)	31.5 (27.8–33.5)	30.2 (28.4–31.7)	0.067
	cVolume (cm ³)	44.1 (15.2–260.1)	70.1 (42.7–147)	0.007
		N = 11	N = 14	
	$\lambda 1$ (*10 ⁻³ mm ² /s)	2.06 (1.61–2.44)	2.12 (2.01–2.39)	0.31
	$\lambda 2$ (*10 ⁻³ mm ² /s)	1.45 (1.06–1.68)	1.43 (1.31–1.67)	0.83
	$\lambda 3$ (*10 ⁻³ mm ² /s)	1.22 (0.91–1.35)	1.22 (1.08–1.36)	0.37
	MD (*10 ⁻³ mm ² /s)	1.59 (1.21–1.78)	1.59 (1.49–1.82)	0.66
FA (–)	0.28 (0.22–0.35)	0.28 (0.23–0.38)	0.85	
Biceps brachii		N (FF/qT2) = 13/12	N = 15	
	Fat fraction (%)	14.4 (4.3–63.9)*	7.6 (6.6–9.9)	0.009
	Water T2 (ms)	29.9 (28.0–34.7)	29.4 (28.2–30.7)	0.063
	cVolume (cm ³)	107 (15.2–245)	153 (79–218)	0.05
		N = 9	N = 12	
	$\lambda 1$ (*10 ⁻³ mm ² /s)	1.96 (1.77–2.25)	2.06 (1.81–2.17)	0.29
	$\lambda 2$ (*10 ⁻³ mm ² /s)	1.37 (1.23–1.64)	1.38 (1.23–1.53)	0.78
	$\lambda 3$ (*10 ⁻³ mm ² /s)	1.18 (0.77–1.3)	1.19 (1.09–1.32)	0.433
	MD (*10 ⁻³ mm ² /s)	1.51 (1.26–1.7)	1.55 (1.44–1.66)	0.7
FA (–)	0.28 (0.23–0.37)	0.29 (0.23–0.34)	0.75	
Triceps brachii		N (FF/qT2) = 13/12	N = 15	
	Fat fraction (%)	33.4 (5.3–72.2)*	6.6 (5.9–9.3)	0.0001
	Water T2 (ms)	30 (27.9–39.8)	29.4 (28.1–30.6)	0.56
	cVolume (cm ³)	124.1 (26.8–270.9)	297.9 (161–568.7)	0.0003
		N = 7	N = 14	
	$\lambda 1$ (*10 ⁻³ mm ² /s)	1.95 (1.84–2.09) [#]	2.13 (1.91–2.35)	0.012
	$\lambda 2$ (*10 ⁻³ mm ² /s)	1.53 (1.12–1.61)	1.56 (1.41–1.7)	0.16
	$\lambda 3$ (*10 ⁻³ mm ² /s)	1.18(0.65–1.61) [#]	1.31 (1.21–1/37)	0.032
	MD (*10 ⁻³ mm ² /s)	1.58 (1.24–1.67) [#]	1.68 (1.54–1.86)	0.019
FA (–)	0.26 (0.2–0.47)	0.25 (0.21–0.28)	0.57	

Notes: Median and range for fat fraction, water T2 relaxation times, contractile volume, and diffusion indices in patients with SMA and controls.

Abbreviations: cVolume, contractile muscle volume; FA, fractional anisotropy; MD, mean diffusivity; SMA, spinal muscular atrophy; $\lambda 1$, eigenvalue 1; $\lambda 2$, eigenvalue 2; $\lambda 3$, eigenvalue 3.

Significant differences between patients and controls are marked with an asterisk (*) and trends are indicated with a number sign ([#]).

BR ($Z = -2.69$; $p = 0.007$) muscle of patients with SMA compared with HCs (Table 2). No differences between the groups were detected for water T2 relaxation time (Figure 2) or any of the diffusion indices for all the upper arm muscles (Figure 3). However, slightly lower values for $\lambda 1$ ($Z = -2.5$; $p = 0.01$), $\lambda 3$ ($Z = -2.14$; $p = 0.031$), and MD ($Z = -2.35$; $p = 0.016$) were seen in the TB muscle of patients with SMA compared with HCs (Figure 3). Based only on visual inspection, there were some variations detectable between SMA types across the muscles. Average FFs were highest in SMA type 3a, followed by type 3b and 4 (Figure 4A). This effect was most apparent in the TB muscle. Across the individual muscles, there were no uniform differences in water T2 relaxation times for the SMA types (Figure 4B). A small effect was seen in the diffusion indices between the SMA types across the muscles, with the highest FA values in patients with SMA type 3a (Figure 4C,D).

3.4 | FF distributions within muscles

Variations in FF along the length of the muscle are visualized for a HC, a patient with SMA with low FFs, a patient with SMA with intermediate FFs, and a patient with SMA with high FFs, in Figure 5. FFs were homogeneously distributed in the BB muscle for patients with

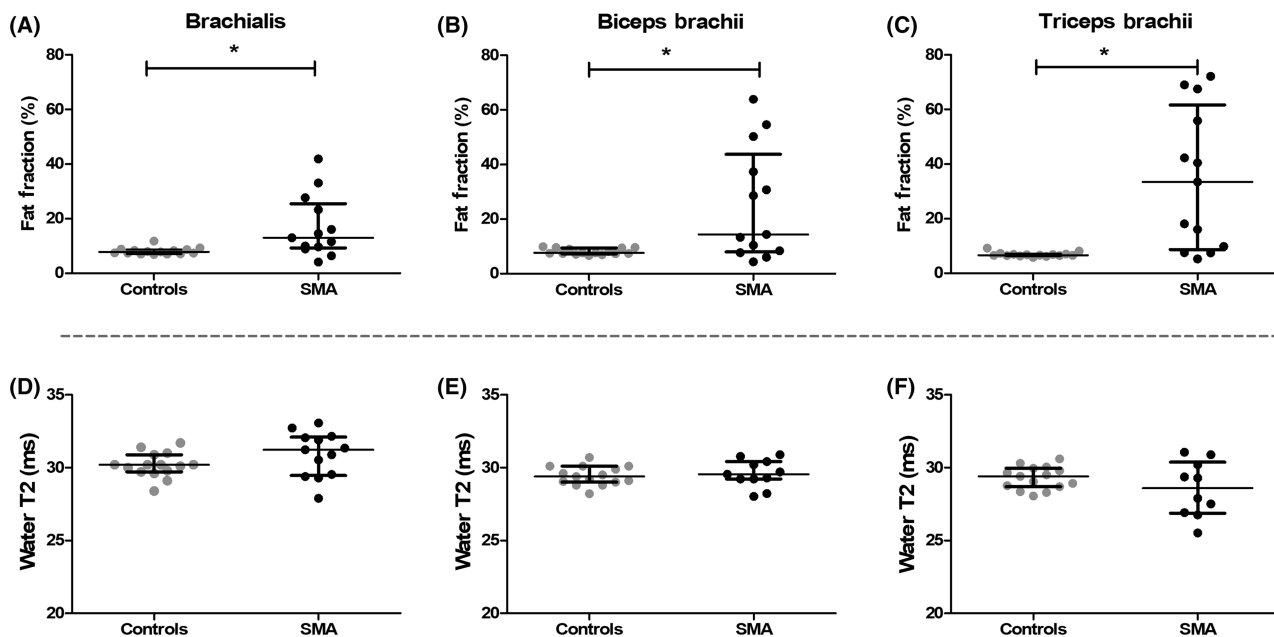


FIGURE 2 Scatter plots showing the individual data points, median, and interquartile range for (A-C) fat fraction and (D-F) water T2 relaxation times in healthy controls (black rounds) and patients with spinal muscular atrophy (SMA) (gray rounds) for the (A) and (D) Brachialis, (B) and (E), Biceps brachii, and (C) and (F) Triceps brachii muscle; *significant group differences: $p < 0.0055$

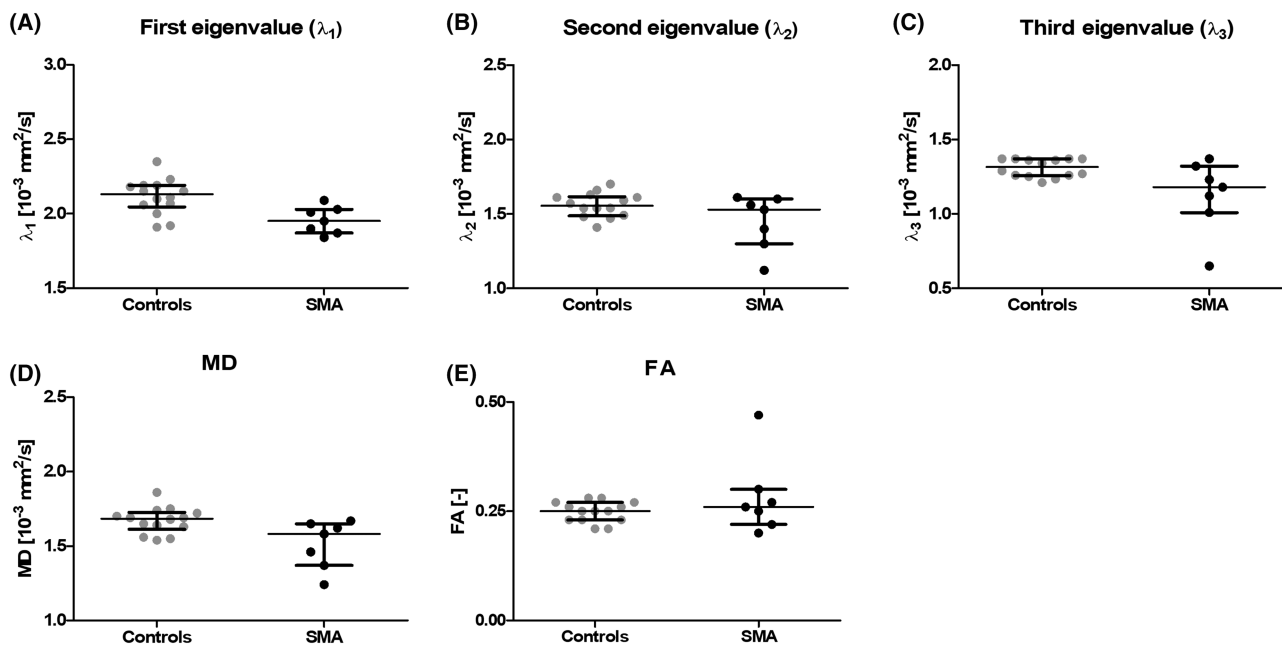


FIGURE 3 Scatter plots showing the individual data points, median, and interquartile range for (D) Mean diffusivity (MD), (E) Fractional anisotropy (FA), and (A-C) the three eigenvalues in healthy controls (black rounds) and patients with spinal muscular atrophy (SMA) (gray rounds) for the triceps brachii muscle; *significant group differences: $p < 0.0055$. Note the trend for a reduction in the first eigenvalue, third eigenvalue, and MD

SMA (chi-square = 5.5; $p = 0.06$), as well as HCs (chi-square = 6; $p = 0.05$) (Figure 6). In the BR muscle of patients with SMA, we found higher FFs proximally compared with the middle ($Z = -3.2$; $p = 0.001$) and distal segments ($Z = -3.2$; $p = 0.001$), whereas in the HCs, a small but significant gradual decline was seen from proximal to distal (dist-mid $Z = -3.2$, $p = 0.001$; prox-dist $Z = -2.73$, $p = 0.006$). In the TB muscle of patients with SMA, FFs gradually increased from distal to middle to proximal, where all segments differed

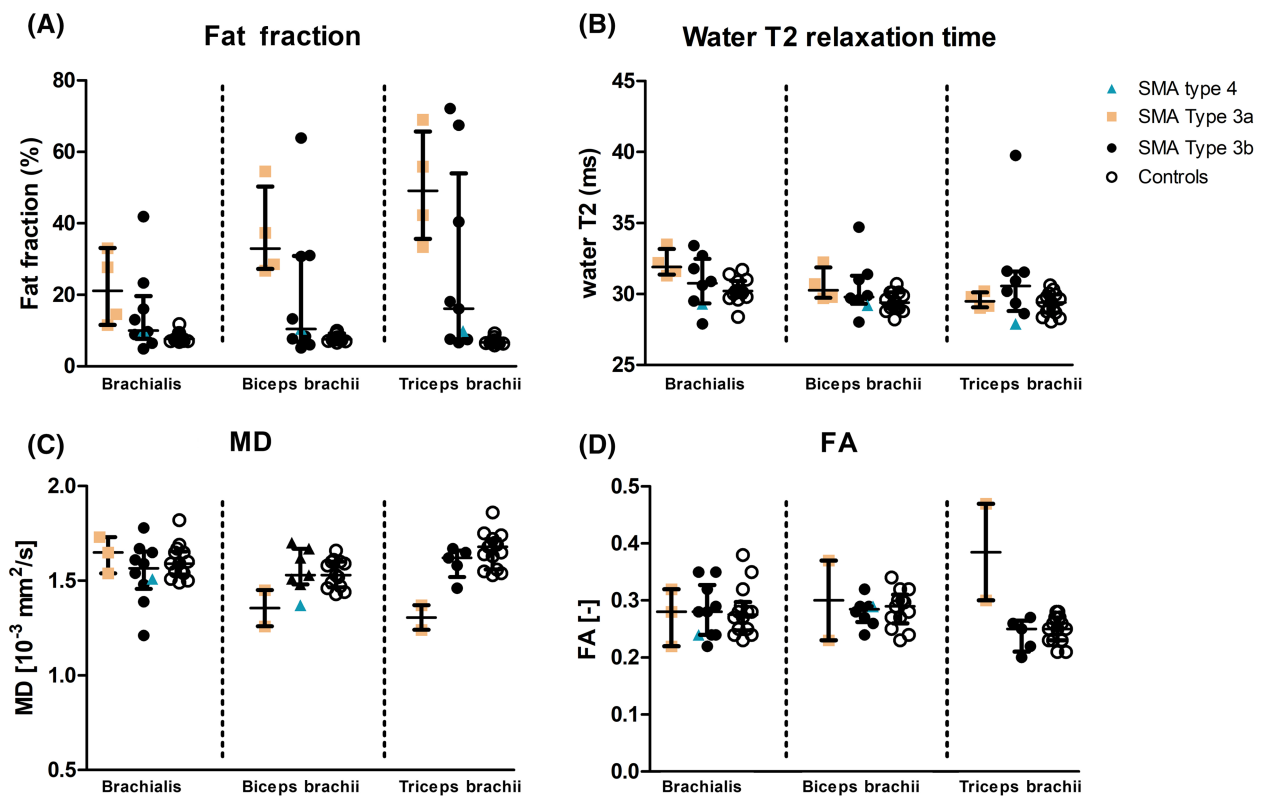


FIGURE 4 Box and whisker plots for (A) The fat fraction, (B) Water T2 relaxation time, (C) Mean diffusivity (MD), and (D) Fractional anisotropy (FA) for the spinal muscular atrophy (SMA) types and healthy controls. SMA type 3a (orange squares); SMA type 3b (black rounds) and 4 (blue triangle) and healthy controls (open rounds). For SMA type 3a, only two diffusion datasets are available of the triceps brachii muscle, resulting in the median being the average of the two data points. The individual data points are presented as red dots

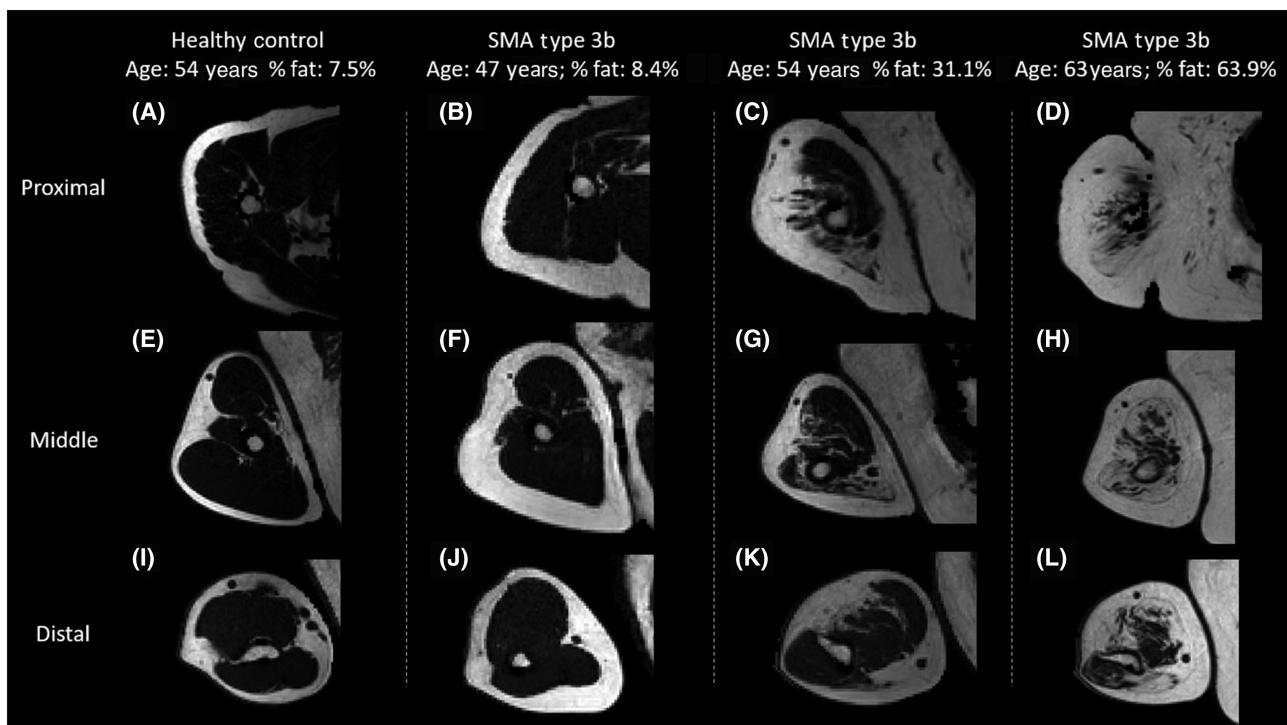


FIGURE 5 Overview of fat distributions within the individual upper arm muscles. Showing a (I–L) Distal, (E–H) Middle, and (A–D) Proximal slice for (A, E and I) A healthy control subject, (B, F and J) A spinal muscular atrophy (SMA) patient with low fat fractions, (C, G and K) A patient with SMA with intermediate fat fractions, and (D, H and L) A patient with SMA with high fat fractions

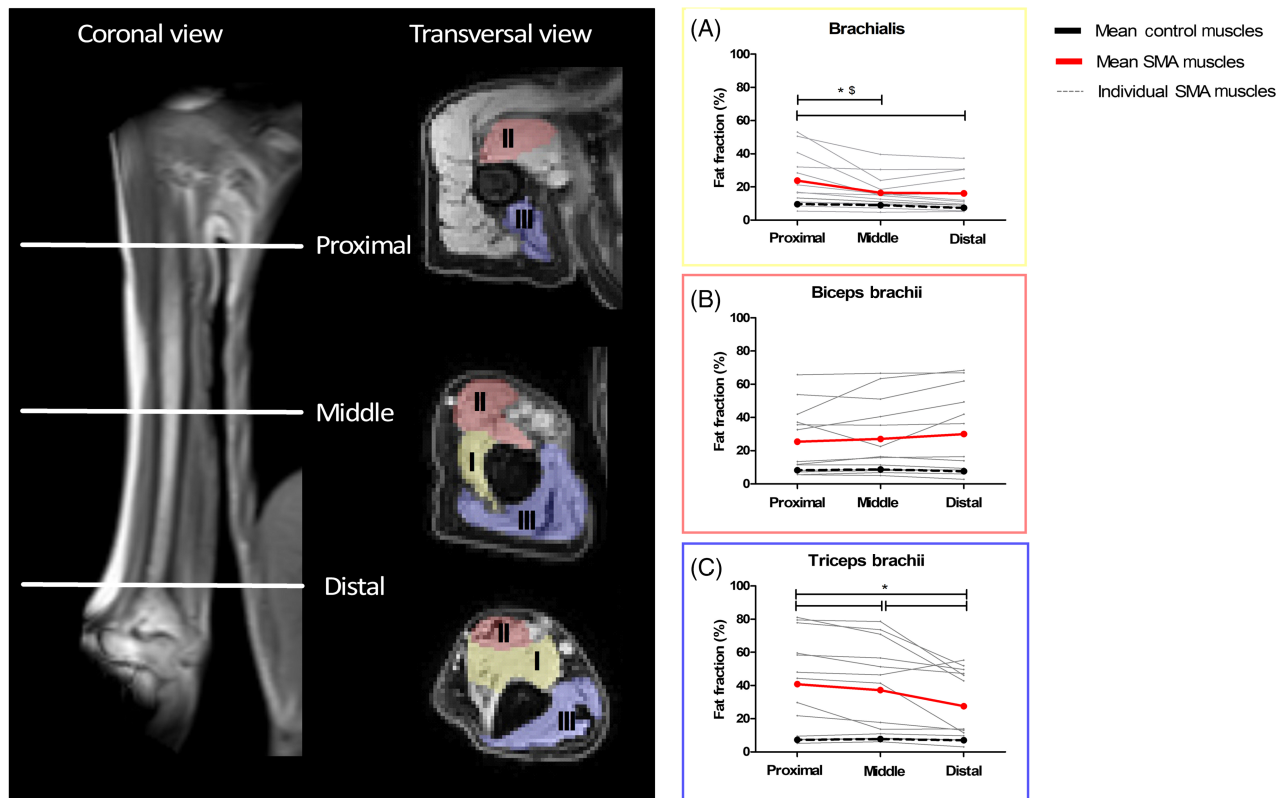


FIGURE 6 Fat distributions within the individual upper arm muscles. The images in the two left columns show a coronal view of the placement of the Dixon field of view used for fat quantification together with axial images representing a distal, middle, and proximal slice with the manual drawn regions of interest (ROIs) for the brachialis (ROI #I – yellow), biceps brachii (ROI #II – red), and triceps brachii (ROI #III – blue) muscle. The line graphs are presented on a muscle-by-muscle basis showing fat fraction in the distal, middle, and proximal segments for the (A) brachialis, (B) biceps brachii and (C) triceps brachii muscle. Individual patients with spinal muscular atrophy (SMA) are plotted in gray, the median value of the SMA patient group is plotted in red, and the median value of the control group in black. Significant differences between segments are indicated with an asterisk (*) for patients with SMA and controls with a dollar sign (\$); p value: 0.0083

(dist-mid $Z = -2.5$; dist-prox $Z = -2.6$; mid-prox $Z = -2.3$; $p < 0.02$), while in HCs, FFs were homogeneously distributed (chi-square = 5.3; $p = 0.071$).

3.5 | Associations of MR outcome measures with MVCF and HFMSE in patients with SMA

We found a weak-to-moderate negative association for both MVCF and HFMSE score with FF in flexor (BR and BB) and TB muscles (Figures 7 and 8). A strong positive association was found between MVCF and MD in the TB muscle but not in the flexor (BR and BB) muscles or with FA (Figure 7). Furthermore, we found a strong positive association of MD and a strong negative association of FA with HFMSE score in the TB muscle (Figure 8). Water T2 relaxation time was negatively associated with HFMSE score in the BR and BB muscle, but not in the TB muscle or with MVCF (Figure 8). Lastly, we found no association between FF and age in the patients with SMA (Figure S1).

4 | DISCUSSION

We used a multi-parametric qMR approach to assess FF, diffusion indices, and water T2 relaxation time in the upper arm muscles of patients with SMA and HCs. Our results show that FFs were significantly higher in all the upper arm muscles of the patients with SMA compared with HCs and were negatively associated with function measures. Additionally, in patients with SMA, FFs were heterogeneously distributed within the TB and BR muscle, whereas FFs were homogeneously distributed in the BB muscle. We did not find differences between patients with SMA and HCs based on the DTI indices or water T2 relaxation time.

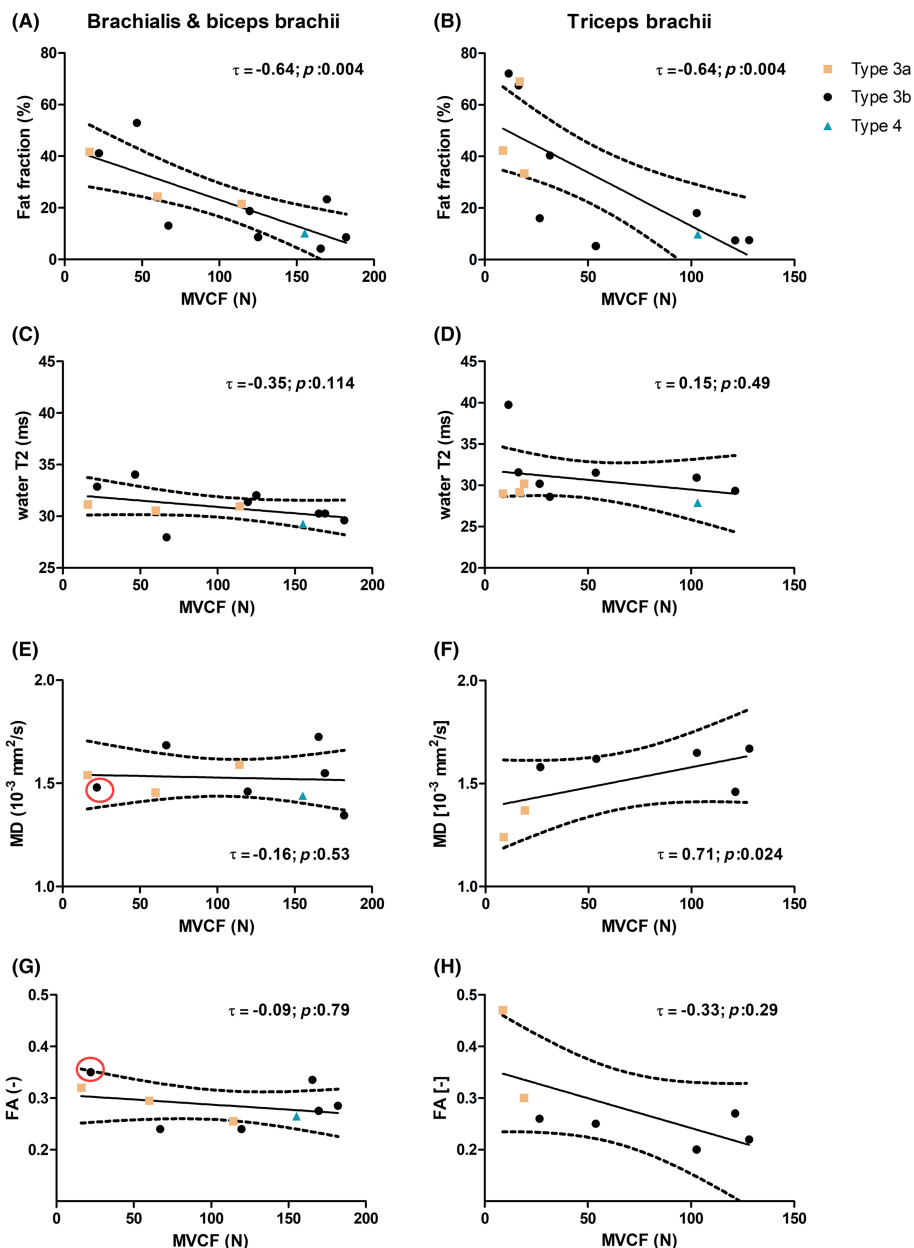


FIGURE 7 The associations between quantitative magnetic resonance imaging (qMRI) measures and maximal voluntary contraction force (MVCF) in patients with spinal muscular atrophy (SMA). (A and B) Fat fraction, (C and D) Mean diffusivity (MD), (E and F) Fractional anisotropy (FA), and (G and H) Water T2 relaxation times are plotted against MVCF of the flexor muscles (A, C, E and G) brachialis and biceps brachii muscle together and (B, D, F and H) triceps brachii muscle. For the flexor muscles, the qMRI measures are an average of the biceps brachii and brachialis for each patient. Linear regression lines with the 95% confidence intervals are plotted in black solid and dotted lines. SMA types are identified by color and sign (i.e. SMA type 3a – orange square; SMA type 3b – black round; SMA type 4 – blue triangle). For one of the subjects, we only have diffusion indices in the brachialis muscle due to high fat fraction in the biceps brachii muscle. The association between MVCF and the diffusion indices for this subject is indicated with a red circle. The Kendall's tau correlation coefficient and the p value are shown per plot

4.1 | FF between and within individual arm muscles

FF was higher in patients with SMA compared with HCs in all upper arm muscles, with the highest FFs in the TB muscle, followed by the BB and BR muscle. We also found variations in FF between SMA types, with the highest FF in SMA type 3a followed by type 3b and 4, which is in line with the clinical presentation of the SMA phenotype. The observed pattern of selective involvement of individual upper arm muscles is in agreement with previous observations.^{14,15,38–40} This selective involvement of muscles is a hallmark of SMA, for which the underlying mechanism is not completely understood. Nevertheless, various hypotheses exist regarding the role of specific biomechanical or anatomical features in this

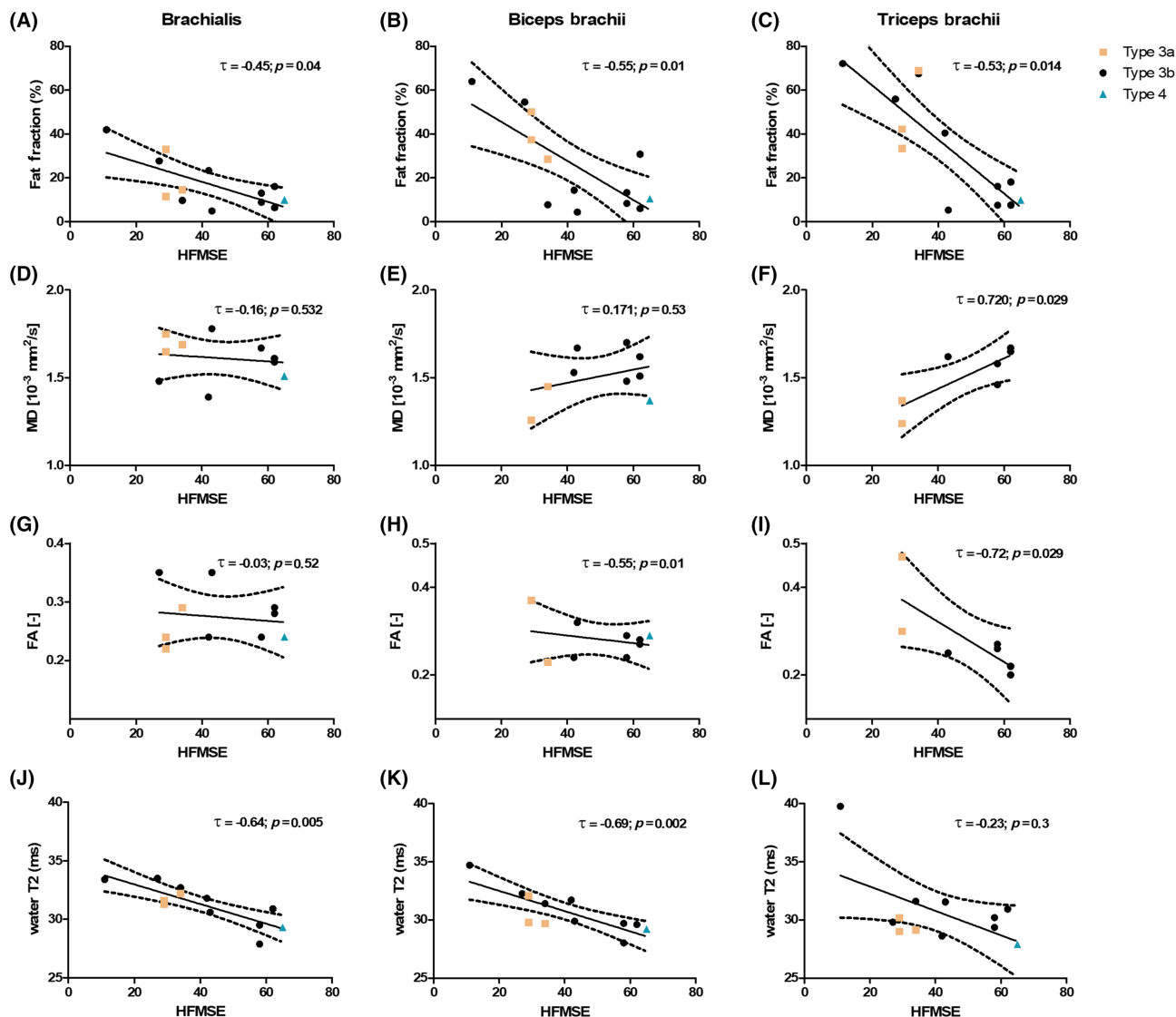


FIGURE 8 The association between quantitative magnetic resonance imaging (qMRI) measures and Hammersmith Functional Motor Scale Expanded (HFME) sum score in patients with spinal muscular atrophy (SMA). (A–C) Fat fraction, (D–F) Mean diffusivity (MD), (G–I) Fractional anisotropy (FA), and (J–L) Water T2 relaxation time are plotted against HFME score for (A, D, G and J) The brachialis, (B, E, H and K) Biceps brachii, and (C, F, I and L) Triceps brachii muscle. The linear regression lines with the 95% confidence intervals are plotted in black solid and dotted lines. SMA types are identified by color and sign (i.e. SMA type 3a – orange square; SMA type 3b – black round; SMA type 4 – blue triangle). The Kendall's tau correlation coefficient and the *p* value are shown per plot

selective vulnerability.^{5,41–43} We also observed variations in FF within individual upper arm muscles of patients with SMA. In two of the muscles (i.e. TB and BR muscle), the highest FFs were detected proximally, whereas the BB muscle showed a homogeneous distribution.^{5,44} This phenomenon has not been reported before in SMA, but has been described in DMD,^{23,45} BMD,²⁶ and FSHD.²⁵ These diseases showed different distributions, that is, in DMD higher FFs were seen in the muscle end segments compared with the muscle belly, in BMD no clear pattern was observed, whereas in FSHD a gradual increase was seen from proximal to distal. Interestingly, in DMD and FSHD,^{23–25} all muscles showed a similar distribution pattern, while we observed between muscle variations in FF distributions along the length of the muscle in patients with SMA. We have no explanation for this heterogeneity between and within muscles. As a next step, it would be of interest to investigate whether this distribution of the FFs is also visible in other muscles or muscle groups and ultimately to investigate the underlying mechanism. FF measurements have proven to be valuable for characterizing muscle involvement and thereby disease status in patients with SMA. Recent longitudinal studies even showed that it is possible to map the slow progressiveness of the disease, reflected by increased FFs, over a period of 6–12 months.^{11,16,20} However, the irreversible nature of the replacement of muscle tissue by fat makes this measure more appropriate for evaluations of future interventions aiming to preserve rather than improve muscle tissue. Other outcome parameters that can reflect the quality of remaining or non-fatty replaced muscle tissue, such as DTI, T2 mapping, and phosphorous spectroscopy (³¹P MRS), might be more suitable for this.

4.2 | Diffusion indices

The mean reported values for the diffusion indices are in the range of values normally expected in skeletal muscle.^{46,47} After correction for multiple comparisons and exclusion of datasets with artefacts, low SNR levels, and high FFs (>50%), we did not find significant changes in diffusion indices between patients with SMA and HCs. However, in our small cohort, we observed a trend towards a reduction in the first eigenvalue, third eigenvalue, and MD in the TB muscle of patients with SMA compared with HCs. We suggest that the latter may be explained by a more advanced disease stage in the TB muscle, indicated by high levels of FF, likely associated with higher levels of myofiber atrophy. The absence of differences in the diffusion indices in the other arm muscles may be explained by a mixture of atrophic and hypertrophic fibers, which was previously observed in muscle biopsy studies in SMA.⁴⁸ Fiber atrophy and hypertrophy have opposing effects on water diffusivity and could therefore average out an effect on the diffusion indices. Our DTI observations in the arm muscles are partly in line with recent work in the thigh muscles of patients with SMA, showing a reduction in MD and an increase in FA in comparison with HCs that has been attributed to myofiber atrophy.¹² Because the DTI assessment by Otto and colleagues focused on MD and FA, a comparison of the eigenvalues is unfortunately not possible. The more pronounced changes detected in the thigh muscles may be due to superior statistical power caused by a combination of a larger sample size in the previous cohort study and the approach of analyzing muscle groups rather than individual muscles. Our results suggest convergence with previous findings in thigh muscles and underline the potential of DTI for mapping disease progression in the remaining and/or non-fatty replaced muscle tissue. Studies with a larger sample size and distinction between non-fatty replaced muscle and low-fat muscles, like the study of Rehmann and colleagues in patients with Pompe disease,⁴⁹ are needed to fully explore the potential of DTI as an outcome measure in neuromuscular diseases, including in SMA.

4.3 | Water T2 relaxation time

We did not detect differences in water T2 relaxation time in any of the upper arm muscles of patients with SMA compared with HCs. This is partly in line with our expectations, as inflammatory changes are not a hallmark of SMA, in contrast to other neuromuscular disorders such as DMD.⁵⁰⁻⁵² However, water T2 relaxation times are not only sensitive to inflammation but also to other pathophysiological processes, although no effect was found here. Nonetheless, global T2 relaxation times and water T2 relaxation times have previously been measured in patients with SMA in the lower leg, upper leg, and upper arm muscles.^{12,19,20} In these studies, various postprocessing algorithms were used to calculate global T2 and water T2 relaxation times, which complicates any comparison of values between studies.⁵³ Longer water T2 relaxation times (ranging from 33.4 to 36.7 ms) were measured by Chabanon and colleagues¹⁹ in the upper arm muscles of patients with SMA using a tri-exponential model for T2 calculation, while Otto and colleagues used the same EPG approach in a study on thigh muscles and found slightly shorter water T2 relaxation times.¹² These shorter relaxation times in highly fat-infiltrated muscles have also been detected in other neuromuscular disorders using spectroscopy and have been attributed to partial volume effects caused by the amount of fat infiltration.^{35,54} Not finding clear group differences in our study in combination with mixed findings in previous studies suggests that water T2 relaxation time is not a meaningful outcome measure for mapping disease status in the arm muscles of patients with SMA.

4.4 | Associations of qMRI parameters with MVCF and HFMSE in patients with SMA

We found the strongest association between FF and MVCF in the most severely affected muscle (i.e. TB muscle). This is in line with previous studies in patients with SMA and suggests a clear relationship between muscle function and FF.^{15,19} The relationship between fat and function in this patient cohort has been investigated in more detail by Habets et al., who reported a strong positive correlation between contractile Cross Sectional Area (cCSA) and MVCF in the TB and BB muscle that did not vary between HCs and patients with SMA.²⁹ This suggests that the force-generating capacity of the remaining muscle tissue is unaffected in patients with SMA. Furthermore, comparable relations between CSA, cCSA, and % fat have been observed in the lower extremity muscles of patients with SMA.¹² Remarkable is the large variation we found in MVCF in the flexor muscles in patients with SMA type 3a but not in the TB muscle or in the HFMSE score. The latter emphasizes the importance of investigating muscle-specific parameters, complementary to overall muscle function. We also observed strong negative correlations for MD with MVCF and HFMSE score in the TB muscle, but not in the other two arm muscles. This finding is partly in line with correlations found in thigh muscles¹² and indicates the potential of diffusion indices as an outcome measure reflecting changes in the remaining muscle tissue. The lack of association between diffusion indices and function measures in the other arm muscles can be explained by the overall lower vulnerability of these muscles in SMA. A moderate negative association of water T2 relaxation time with HFMSE score was observed in the BR and BB muscle, but not in the TB muscle or with MVCF. We have no explanation for the latter; however, it suggests a potential relationship with overall function that should be explored in future studies with larger cohorts.

4.5 | Limitations

The small number of patients with SMA participating in this explorative observational study was highly heterogeneous in age and disease severity, which precludes definite conclusions. Some of the DTI datasets had to be discarded due to insufficient quality as a result of extensive fat replacement, fat artefacts, and low SNR. This resulted in some bias to less severely affected muscles and could explain the absence of significant differences in DTI indices. For future applications, other shimming strategies and positions for the upper arm could be explored to improve shimming, which could benefit the fat suppression. In addition, more averages could be obtained for higher SNR, but the longer scan times would reduce the clinical applicability of the measurement. These strategies may benefit data acquisition in HCs, slightly and intermediately affected patients. However, in severely affected patients, it is unavoidable that some data must be excluded, because of low SNR/high fat, as in these cases almost no muscle tissue is left. The Dixon FOV did not cover the full length of the upper arm muscles. Therefore, variations seen along the length of the individual upper arm muscles could have been slightly underestimated or overestimated. Nevertheless, our study showed the feasibility of upper arm qMRI in SMA and indicates its potential. Future studies should aim to obtain data of complete muscle volumes, to verify any observations of heterogeneity in the FF of individual muscles. We also need to collect longitudinal data to confirm and further explore the use of qMRI to map disease state, progression, and to detect the early effects of interventions.

4.6 | Conclusion

Our multi-parametricMR approach showed that it is feasible to quantitatively map disease state in the upper arm muscles of patients with SMA over a wide range of disease phases. Two- to 5-fold higher FFs were measured in the upper arm muscles of patients with SMA compared with HCs, with clear differences between and within individual muscles. No differences were detected in water T2 relaxation times, while DTI indices showed potential for mapping changes in the remaining muscle tissue. Additionally, FFs in all three upper arm muscles and MD in the TB muscle were associated with function measures in patients with SMA.

ORCID

Melissa T. Hooijmans  <https://orcid.org/0000-0002-2233-1383>

Martijn Froeling  <https://orcid.org/0000-0003-3841-0497>

REFERENCES

- Lefebvre S, Burglen L, Reboullet S, et al. Identification and characterization of a spinal muscular atrophy-determining gene. *Cell*. 1995;80(1):155-165. doi:10.1016/0092-8674(95)90460-3
- D'Amico A, Mercuri E, Tiziano FD, Bertini E. Spinal muscular atrophy. *Orphanet J Rare Dis*. 2011;6:71. doi:10.1186/1750-1172-6-71
- Goulet BB, Kothary R, Parks RJ. At the "junction" of spinal muscular atrophy pathogenesis: the role of neuromuscular junction dysfunction in SMA disease progression. *Curr Mol Med*. 2013;13(7):1160-1174. doi:10.2174/15665240113139990044
- Wadman RI, Wijngaarde CA, Stam M, et al. Muscle strength and motor function throughout life in a cross-sectional cohort of 180 patients with spinal muscular atrophy types 1c-4. *Eur J Neurol*. 2018;25(3):512-518. doi:10.1111/ene.13534
- Wadman RI, Stam M, Gijzen M, et al. Association of motor milestones, SMN2 copy and outcome in spinal muscular atrophy types 0-4. *J Neurol Neurosurg Psychiatry*. 2017;88(4):365-367. doi:10.1136/jnnp-2016-314292
- Munsat TL, Davies KE. International SMA consortium meeting. (26-28 June 1992, Bonn, Germany). *Neuromuscul Disord*. 1992;2(5-6):423-428. doi:10.1016/s0960-8966(06)80015-5
- Mercuri E, Darras BT, Chiriboga CA, et al. Nusinersen versus sham control in later-onset spinal muscular atrophy. *N Engl J Med*. 2018;378(7):625-635. doi:10.1056/NEJMoa1710504
- Groen EJM, Talbot K, Gillingwater TH. Advances in therapy for spinal muscular atrophy: promises and challenges. *Nat Rev Neurol*. 2018;14(4):214-224. doi:10.1038/nrneurol.2018.4
- Yeo CJJ, Darras BT, Yeo and Darras: extraneuronal phenotypes of spinal muscular atrophy. *Ann Neurol*. 2021;89(1):24-26. doi:10.1002/ana.25930
- Strijkers GJ, Araujo ECA, Azzabou N, et al. Exploration of New Contrasts, Targets, and MR Imaging and Spectroscopy Techniques for Neuromuscular Disease - A Workshop Report of Working Group 3 of the Biomedicine and Molecular Biosciences COST Action BM1304 MYO-MRI. *J Neuromuscul Dis*. 2019;6(1):1-30. doi:10.3233/JND-180333
- Otto LAM, Froeling M, van Eijk RPA, et al. Quantification of disease progression in spinal muscular atrophy with muscle MRI—a pilot study. *NMR Biomed*. 2021;34(4):e4473. doi:10.1002/nbm.4473
- Otto LAM, van der Pol WL, Schaffke L, et al. Quantitative MRI of skeletal muscle in a cross-sectional cohort of patients with spinal muscular atrophy types 2 and 3. *NMR Biomed*. 2020;33(10):e4357. doi:10.1002/nbm.4357
- Brogna C, Cristiano L, Verdolotti T, et al. Predominant distal muscle involvement in spinal muscular atrophy. *Neuromuscul Disord*. 2019;29(11):910-911. doi:10.1016/j.nmd.2019.09.002
- Brogna C, Cristiano L, Verdolotti T, et al. MRI patterns of muscle involvement in type 2 and 3 spinal muscular atrophy patients. *J Neurol*. 2020;267(4):898-912. doi:10.1007/s00415-019-09646-w

15. Durmus H, Yilmaz R, Gulsen-Parman Y, et al. Muscle magnetic resonance imaging in spinal muscular atrophy type 3: Selective and progressive involvement. *Muscle Nerve*. 2017;55(5):651-656. doi:10.1002/mus.25385
16. Sproule DM, Montgomery MJ, Punyanitya M, et al. Thigh muscle volume measured by magnetic resonance imaging is stable over a 6-month interval in spinal muscular atrophy. *J Child Neurol*. 2011;26:1252-1259. doi:10.1177/0883073811405053
17. Sproule DM, Punyanitya M, Shen W, et al. Muscle volume estimation by magnetic resonance imaging in spinal muscular atrophy. *J Child Neurol*. 2011;26(3):309-317. doi:10.1177/0883073810380457
18. Leroy-Willig A, Willig TN, Henry-Feugeas MC, et al. Body composition determined with MR in patients with Duchenne muscular dystrophy, spinal muscular atrophy, and normal subjects. *Magn Reson Imaging*. 1997;15(7):737-744. doi:10.1016/s0730-725x(97)00046-5
19. Chabanon A, Seferian AM, Daron A, et al. Prospective and longitudinal natural history study of patients with Type 2 and 3 spinal muscular atrophy: Baseline data NatHis-SMA study. *PLoS One*. 2018;13(7):e0201004. doi:10.1371/journal.pone.0201004
20. Bonati U, Holiga S, Hellbach N, et al. Longitudinal characterization of biomarkers for spinal muscular atrophy. *Ann Clin Transl Neurol*. 2017;4(5):292-304. doi:10.1002/acn3.406
21. Kruitwagen-van Reenen ET, van der Pol L, Schroder C, et al. Social participation of adult patients with spinal muscular atrophy: Frequency, restrictions, satisfaction, and correlates. *Muscle Nerve*. 2018;58(6):805-811. doi:10.1002/mus.26201
22. Kruitwagen-Van Reenen ET, Wadman RI, Visser-Meily JM, van den Berg LH, Schroder C, van der Pol WL. Correlates of health related quality of life in adult patients with spinal muscular atrophy. *Muscle Nerve*. 2016;54(5):850-855. doi:10.1002/mus.25148
23. Hooijmans MT, Niks EH, Burakiewicz J, et al. Non-uniform muscle fat replacement along the proximodistal axis in Duchenne muscular dystrophy. *Neuromuscul Disord*. 2017;27(5):458-464. doi:10.1016/j.nmd.2017.02.009
24. Chrzanowski SM, Baligand C, Willcocks RJ, et al. Multi-slice MRI reveals heterogeneity in disease distribution along the length of muscle in Duchenne muscular dystrophy. *Acta Myol*. 2017;36(3):151-162.
25. Janssen BH, Voet NB, Nabuurs CI, et al. Distinct disease phases in muscles of facioscapulohumeral dystrophy patients identified by MR detected fat infiltration. *PLoS One*. 2014;9(1):e85416. doi:10.1371/journal.pone.0085416
26. van de Velde NM, Hooijmans MT, Sardjoe Mishre ASD, et al. Selection approach to identify the optimal biomarker using quantitative muscle MRI and functional assessments in Becker muscular dystrophy. *Neurology*. 2021;97(5):e513-e522. doi:10.1212/WNL.0000000000012233
27. Wijngaarde CA, Stam M, Otto LAM, et al. Muscle strength and motor function in adolescents and adults with spinal muscular atrophy. *Neurology*. 2020;95(14):e1988-e1998. doi:10.1212/WNL.0000000000010540
28. Habets LE, Bartels B, Asselman F, et al. Magnetic resonance spectroscopy reveals mitochondrial dysfunction and remodeling in spinal muscular atrophy. *Brain*. 2021;awab411. doi:10.1093/brain/awab411
29. Habets LE, Bartels B, Asselman FL, et al. Magnetic resonance reveals mitochondrial dysfunction and muscle remodelling in spinal muscular atrophy. *Brain*. 2021;awab411. doi:10.1093/brain/awab411
30. Reeder SB, Pineda AR, Wen Z, et al. Iterative decomposition of water and fat with echo asymmetry and least-squares estimation (IDEAL): application with fast spin-echo imaging. *Magn Reson Med*. 2005;54(3):636-644. doi:10.1002/mrm.20624
31. Klein S, Staring M, Murphy K, Viergever MA, Pluim JP. elastix: a toolbox for intensity-based medical image registration. *IEEE Trans Med Imaging*. 2010;29(1):196-205. doi:10.1109/TMI.2009.2035616
32. De Luca A, Bertoldo A, Froeling M. Effects of perfusion on DTI and DKI estimates in the skeletal muscle. *Magn Reson Med*. 2017;78(1):233-246. doi:10.1002/mrm.26373
33. Froeling M, Nederveen AJ, Nicolay K, Strijkers GJ. DTI of human skeletal muscle: the effects of diffusion encoding parameters, signal-to-noise ratio and T2 on tensor indices and fiber tracts. *NMR Biomed*. 2013;26:1339-1352. doi:10.1002/nbm.2959
34. Williams SE, Heemskerk AM, Welch EB, Li K, Damon BM, Park JH. Quantitative effects of inclusion of fat on muscle diffusion tensor MRI measurements. *J Magn Reson Imaging*. 2013;38(5):1292-1297. doi:10.1002/jmri.24045
35. Keene KR, Beenakker JWM, Hooijmans MT, et al. T-2 relaxation-time mapping in healthy and diseased skeletal muscle using extended phase graph algorithms. *Magn Reson Med*. 2020;84(5):2656-2670. doi:10.1002/mrm.28290
36. Marty B, Baudin PY, Reyngoudt H, et al. Simultaneous muscle water T2 and fat fraction mapping using transverse relaxometry with stimulated echo compensation. *NMR Biomed*. 2016;29(4):431-443. doi:10.1002/nbm.3459
37. Yushkevich PA, Piven J, Hazlett HC, et al. User-guided 3D active contour segmentation of anatomical structures: significantly improved efficiency and reliability. *Neuroimage*. 2006;31(3):1116-1128. doi:10.1016/j.neuroimage.2006.01.015
38. Liu GC, Jong YJ, Chiang CH, Yang CW. Spinal muscular atrophy: MR evaluation. *Pediatr Radiol*. 1992;22(8):584-586. doi:10.1007/BF02015357
39. Mercuri E, Pichiecchio A, Allsop J, Messina S, Pane M, Muntoni F. Muscle MRI in inherited neuromuscular disorders: past, present, and future. *J Magn Reson Imaging*. 2007;25(2):433-440. doi:10.1002/jmri.20804
40. Quijano-Roy S, Avila-Smirnow D, Carlier RY, group W-Mms. Whole body muscle MRI protocol: pattern recognition in early onset NM disorders. *Neuromuscul Disord*. 2012;22(Suppl 2):S68-S84. doi:10.1016/j.nmd.2012.08.003
41. Piepers S, van der Pol WL, Brugman F, Wokke JH, van den Berg LH. Natural history of SMA IIIb: muscle strength decreases in a predictable sequence and magnitude. *Neurology*. 2009;72(23):2057-2058; author reply 2058. doi:10.1212/01.wnl.0000349698.94744.1e
42. Mentis GZ, Blivis D, Liu W, et al. Early functional impairment of sensory-motor connectivity in a mouse model of spinal muscular atrophy. *Neuron*. 2011;69(3):453-467. doi:10.1016/j.neuron.2010.12.032
43. Deymeer F, Serdaroglu P, Poda M, Gulsen-Parman Y, Ozcelik T, Ozdemir C. Segmental distribution of muscle weakness in SMA III: implications for deterioration in muscle strength with time. *Neuromuscul Disord*. 1997;7(8):521-528. doi:10.1016/s0960-8966(97)00113-2
44. Piepers S, van den Berg LH, Brugman F, et al. A natural history study of late onset spinal muscular atrophy types 3b and 4. *J Neurol*. 2008;255(9):1400-1404. doi:10.1007/s00415-008-0929-0
45. Spitali P, Hettne K, Tsonaka R, et al. Tracking disease progression non-invasively in Duchenne and Becker muscular dystrophies. *J Cachexia Sarcopenia Muscle*. 2018;9(4):715-726. doi:10.1002/jcsm.12304
46. Monte JR, Hooijmans MT, Froeling M, et al. The repeatability of bilateral diffusion tensor imaging (DTI) in the upper leg muscles of healthy adults. *Eur Radiol*. 2020;30(3):1709-1718. doi:10.1007/s00330-019-06403-5
47. Schlaffke L, Rehmann R, Rohm M, et al. Multi-center evaluation of stability and reproducibility of quantitative MRI measures in healthy calf muscles. *NMR Biomed*. 2019;32(9):e4119. doi:10.1002/nbm.4119

48. Dubowitz V. *Muscle Biopsy*. 3rd edition ed. Saunders Elsevier; 2007.
49. Rehmann R, Froeling M, Rohm M, et al. Diffusion tensor imaging reveals changes in non-fat infiltrated muscles in late onset Pompe disease. *Muscle Nerve*. 2020;62(4):541-549. doi:[10.1002/mus.27021](https://doi.org/10.1002/mus.27021)
50. Forbes SC, Willcocks RJ, Triplett WT, et al. Magnetic resonance imaging and spectroscopy assessment of lower extremity skeletal muscles in boys with Duchenne muscular dystrophy: a multicenter cross sectional study. *PLoS One*. 2014;9(9):e106435. doi:[10.1371/journal.pone.0106435](https://doi.org/10.1371/journal.pone.0106435)
51. Hooijmans MT, Niks EH, Burakiewicz J, Verschuuren JJ, Webb AG, Kan HE. Elevated phosphodiester and T2 levels can be measured in the absence of fat infiltration in Duchenne muscular dystrophy patients. *NMR Biomed*. 2017;30(1):e3667. doi:[10.1002/nbm.3667](https://doi.org/10.1002/nbm.3667)
52. Wood CL, Hollingsworth KG, Hughes E, et al. Pubertal induction in adolescents with DMD is associated with high satisfaction, gonadotropin release and increased muscle contractile surface area. *Eur J Endocrinol*. 2021;184(1):67-79. doi:[10.1530/EJE-20-0709](https://doi.org/10.1530/EJE-20-0709)
53. Carlier PG. Global T2 versus water T2 in NMR imaging of fatty infiltrated muscles: different methodology, different information and different implications. *Neuromuscul Disord*. 2014;24(5):390-392. doi:[10.1016/j.nmd.2014.02.009](https://doi.org/10.1016/j.nmd.2014.02.009)
54. Schlaeger S, Weidlich D, Klupp E, et al. Decreased water T2 in fatty infiltrated skeletal muscles of patients with neuromuscular diseases. *NMR Biomed*. 2019;32(8):e4111. doi:[10.1002/nbm.4111](https://doi.org/10.1002/nbm.4111)

SUPPORTING INFORMATION

Additional supporting information may be found in the online version of the article at the publisher's website.

How to cite this article: Hooijmans MT, Habets LE, van den Berg-Faay SAM, et al. Multi-parametric quantitative magnetic resonance imaging of the upper arm muscles of patients with spinal muscular atrophy. *NMR in Biomedicine*. 2022;35(7):e4696. doi:[10.1002/nbm.4696](https://doi.org/10.1002/nbm.4696)